VI International Conference on Computational Methods for Coupled Problems in Science and Engineering
COUPLED PROBLEMS 2015
B. Schrefler, E. Oñate and M. Papadrakakis(Eds)

ANANLYSIS OF ACTUATOR MADE OF FGM USING NEW ELECTRO-THERMO-MECHANICAL FINITE ELEMENTS

JURAJ PAULECH*, JURAJ HRABOVSKÝ*, JUSTÍN MURÍN* AND VLADIMÍR KUTIŠ*

*Department Applied Mechanics and Mechatronics
Institute of Automotive Mechatronics
Faculty of Electrical Engineering and Information Technology
Slovak University of Technology in Bratislava
812 19 Bratislava, Slovak Republic
e-mail: juraj.paulech@stuba.sk, web page: http://www.stuba.sk

Key words: Actuator, coupled electro-thermo-mechanical analysis, Functionally Graded Materials, new FEM equations

Abstract. Actuator is a mechatronic system that transforms one type of energy (e.g. electric energy) into the mechanical displacement and mechanical force (mechanical energy). Nowadays, these actuators can be made of Functionally Graded Materials (FGM) to ensure simple shape of the actuator and to improve its effectiveness, particularly for micro systems. FGM is built as a mixture of two or more constituents which have almost the same geometry and dimensions. The variation of macroscopic material properties can be induced by variation of both the volume fractions and material properties (e.g. by a non-homogeneous temperature field) of the FGM constituents.
The paper deals with a new approach in analysing of the systems made of FGM using our new beam finite elements. Multiphysical analysis (weak coupled electro-thermo-mechanical analysis) and spatial continuous variation of material properties are supported. The analysis of the micro actuator with constant cross section made of FGM is presented in the paper. This simple-shaped actuator is supplied by electric current and the efficiency of the actuator is optimised. The solution results will be compared with those obtained by using solid elements of a FEM commercial program.

1 INTRODUCTION

Nowadays, the scientific and technological progress are already at such level that for the development of new systems in classical way (such as mechanical and heating systems, systems in construction industry, etc.) it is not enough to propose new shapes of components and their optimization, but it requires use of new materials with the desired properties that lie outside the parameters of materials commonly used for that purpose.

New materials like Functionally Graded Material (FGM) are necessary for sophisticated structures like Micro-Electro-Mechanical Systems (MEMS), advanced electronic devices, etc. In all these applications, using new materials like FGM can greatly improve efficiency of a system e.g. classic shape of actuator (Fig. 1a) can be replaced by new type – simply-shaped actuator (Fig. 1b) where functionality is caused by varying material properties.

Figure 1: a) Classic shape of MEMS actuator, b) New shape of FGM actuator

FGM is built as a mixture of two or more constituents which have almost the same geometry and dimensions. From macroscopic point of view, FGM is isotropic in each material point but the material properties can vary continuously or discontinuously in one, two or three directions. The variation of macroscopic material properties can be caused by varying the volume fraction of the constituents or with varying of the constituents' material properties (e.g. by non-homogeneous temperature field). The methods based on the homogenization theory have been designed and successfully applied to determine the effective material properties of heterogeneous materials from the corresponding material behavior of the constituents (and of the interfaces between them) and from the geometrical arrangement of the phases.
Coupled electro-thermo-mechanical analysis of actuator made of FGM using our new beam finite elements will be presented.

2 FEM EQUATIONS FOR COUPLED ELECTRO - THERMO - MECHANICAL ANALYSIS

Derivation process of the new FEM equations for coupled electro-thermo-mechanical element is based on differential equations for electric thermal and structural fields for 1D type of analysis, respectively. All quantities in following equations are the polynomial functions of x. Homogenization process of the varying material properties and the calculation of other effective finite element parameters have been done by extended mixture rule [1] and multilayer method is fully described in [2],[3].

2.1 Differential equations

Homogeneous 1D static differential equation for FGM (with non-constant coefficients on on the left-hand side) for electric field with boundary conditions has a form:

$$\begin{gathered} -\sigma(x)\frac{d^2\varphi(x)}{dx^2} - \frac{d\sigma(x)}{dx}\frac{d\varphi(x)}{dx} = 0 \\ \varphi(0) = \varphi_0 \qquad J(L) = J_L \end{gathered} \tag{1}$$

where $\varphi(x)$ [V] is the electric potential, $\sigma(x)$ [S/m] is the specific electric conductivity and $J(x)$ [Am^{-2}] is the current density.

Static differential equation for heat transfer with non-constant auxiliary thermal source $Q(x)$ [Wm^{-3}] in the volume, with non-constant convective heat transfer coefficient $\alpha_t(x)$ [K^{-1}] and with coupled to the electric field has a form (2). One-way coupling between the electric and thermal field is provided by Joule heat $P_{J1}(x)$ [W/m^3], that can be calculated as one of the outputs from electric analysis and it enters the thermal analysis as volume heat (beside or instead of $Q(x)$).

$$-\lambda(x)\frac{d^2T(x)}{dx^2} - \frac{d\lambda(x)}{dx}\frac{dT(x)}{dx} + \alpha_t(x)T(x)\frac{o}{A} = P_{J1}(x) + Q(x) + \alpha_t(x)T_{amb}\frac{o}{A} \tag{2}$$

with boundary conditions, e.g.:

$$T(0) = 0 \qquad q(L) = q_L \tag{3}$$

where $\lambda(x)$ [Wm^{-1}K^{-1}] is the thermal conductivity, $T(x)$ [K] is the temperature, o [m] is the perimeter, A [m^2] is the cross section area, T_{amb} [K] is the ambient temperature and $q(x)$ [Wm^{-2}] is the heat flux.

Homogeneous differential equation for structural analysis with effect of thermal expansion (coupling with the electro-thermal analysis) for pure tensile and compressive stress has a form:

$$\begin{aligned} &E_L^{NH}(x)\frac{d^2u(x)}{dx^2} + \frac{dE_L^{NH}(x)}{dx}\frac{du(x)}{dx} = \\ &= \frac{n(x)}{A} + \alpha_t(x)\Delta t(x)\frac{dE_L^{NH}(x)}{dx} + \Delta T(x)E_L^{NH}(x)\frac{d\alpha_t(x)}{dx} + E_L^{NH}(x)\alpha_t(x)\frac{d\Delta t(x)}{dx} \end{aligned} \tag{4}$$

with boundary conditions, e.g.:

$$u(0) = u_0 \qquad \sigma_N^s(L) = \sigma_{N,L}^s \tag{5}$$

where $E_L^{NH}(x)$ [Pa] is the Young modulus for tension/compression, $u(x)$ [m] is the displacement, $n(x)$ [Nm^{-1}] are the distributed axial forces, $N(x)$ [N] is the normal force and α_t [K^{-1}] is the coefficient of thermal expansion.

Homogeneous differential equation for structural analysis for bending has a form:

$$\frac{d^2w(x)}{dx^2} = \frac{M(x)}{E_L^{MH}}(x)I_y \tag{6}$$

with boundary conditions, e.g.:

$$w(0) = w_0 \qquad \sigma_y(L) = \sigma_{y,L} \tag{7}$$

where $w(x)$ [m] is the transversal displacement, $M(x)$ is the bending moment, $E_L^{MH}(x)$ is the Young modulus for bending, $\varphi_y(x)$ [rad] is the angle of the cross section rotation (around y axis), I_y [m^4] is the quadratic moment of the cross section.

The solution of these differential equations is based on numerical method for solving 1D differential equation with non-constant coefficients and with right-hand side described in [4] in detail.

2.2 New beam/link FGM finite element equations

The finite element equations for electric analysis in FGM link have a form:

$$\begin{bmatrix} c_0(L) & -1 \\ -\left(c_0(L) - \dfrac{c_1(L)c_0'(L)}{c_1'(L)}\right) & 1 \end{bmatrix} \cdot \begin{bmatrix} \varphi_0 \\ \varphi_L \end{bmatrix} = \begin{bmatrix} \dfrac{c_1(L)}{\sigma_0} J_0 \\ \dfrac{c_1(L)}{c_1'(L)\sigma_L} J_L \end{bmatrix} \tag{8}$$

FEM equations for thermal analysis considering the convective effect, generated heat and Joule heat (coupling between the electric and thermal field) have a form:

$$\begin{bmatrix} c_0(L) & -1 \\ -\left(c_0(L) - \dfrac{c_1(L)c_0'(L)}{c_1'(L)}\right) & 1 \end{bmatrix} \cdot \begin{bmatrix} T_0 \\ T_L \end{bmatrix} =$$

$$= \begin{bmatrix} \dfrac{c_1(L)}{\lambda_0} q_0 - \displaystyle\sum_{j=0}^{g} \varepsilon_j b_{j+2}(L) \\ \dfrac{c_1(L)}{c_1'(L)\lambda_L} q_L - \dfrac{c_1(L)}{c_1'(L)} \displaystyle\sum_{j=0}^{g} \varepsilon_j b_{j+2}'(L) + \displaystyle\sum_{j=0}^{g} \varepsilon_j b_{j+2}(x) \end{bmatrix} \tag{9}$$

Derived FEM equations for the structural analysis for pure tensile and compressive stress with coupling to the electro-thermal analysis (thermal expansion coefficient) have a form:

$$\begin{bmatrix} c_0(L) & -1 \\ -\left(c_0(L) - \dfrac{c_1(L)c_0'(L)}{c_1'(L)}\right) & 1 \end{bmatrix} \cdot \begin{bmatrix} u_0 \\ u_L \end{bmatrix} =$$

$$= \begin{bmatrix} \dfrac{c_1(L)}{E_L^{NH}A} N_0 - c_1(L)\alpha_{t0}\Delta T_0 - \displaystyle\sum_{j=0}^{g} \varepsilon_j b_{j+2}(L) \\ \dfrac{c_1(L)}{c_1'(L)} \left(\dfrac{N_L}{E_L^{NH}A} + \alpha_{tL}\Delta T_L - \displaystyle\sum_{j=0}^{g} \varepsilon_j b_{j+2}'(L) \right) + \displaystyle\sum_{j=0}^{g} \varepsilon_j b_{j+2}(L) \end{bmatrix} \tag{10}$$

and FEM equations for bending of the beam have general form:

$$\begin{bmatrix} K_{11} & K_{12} & K_{13} & K_{14} \\ K_{21} & K_{22} & K_{23} & K_{24} \\ K_{31} & K_{32} & K_{33} & K_{34} \\ K_{41} & K_{42} & K_{43} & K_{44} \end{bmatrix} \cdot \begin{bmatrix} w_0 \\ \varphi_{y,0} \\ w_L \\ \varphi_{y,L} \end{bmatrix} = \begin{bmatrix} T_{z,0} \\ M_0 \\ T_{z,L} \\ M_L \end{bmatrix} \tag{11}$$

where $T_z(x)$ [N] is the transversal force.
The terms $c_i(x)$, c_i', $b_i(x)$, $b_i'(x)$, $i \in \langle 0, 1\rangle$ are the transfer functions (for particular solution and for uniform solution) of the differential equations (1) - (6) which can be calculated by simple numerical algorithm [4].

3 NUMERICAL EXPERIMENT

Let us consider actuator with constant cross section made of FGM according to Fig. 2. It consists of 3 parts (beams) that lengths are: $L_1 = 5$ mm, $L_2 = 0.25$ mm and $L_3 = 5$ mm. Their constant rectangular cross-section is $b = 0.2$ mm and $h = 0.1$ mm.

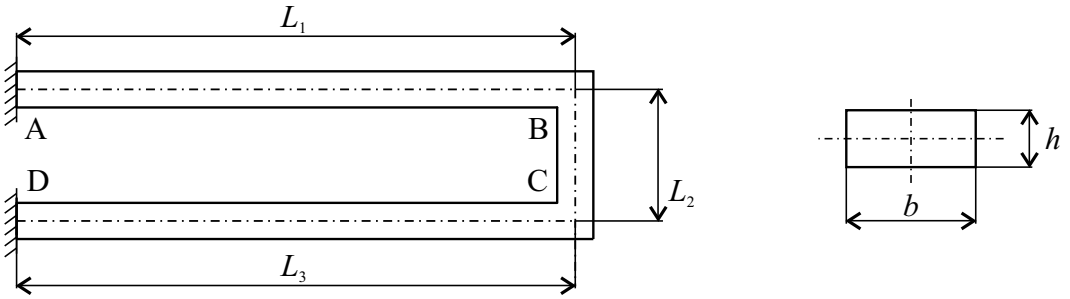

Figure 2: FGM microactuator

Actuator is made of FGM that consist of two components: NiFe - named as matrix and denoted with index m and Tungsten - named as fibre and denoted with index f. Material properties of the components are constant (not temperature dependent): Nife (matrix): Young modulus $E_m = 255$ GPa, thermal conductivity $\lambda_m = 100$ W/mK, electric conductivity $\gamma_m = 1.31 \times 10^7$ S/m, thermal expansion coefficient $\alpha_m = 1.5 \times 10^{-5}$ K^{-1}; Thungsten (fibre): Young modulus $E_f = 400$ GPa, thermal conductivity $\lambda_f = 160$ W/mK, electric conductivity $\gamma_f = 2.84 \times 10^7$ S/m, thermal expansion coefficient $\alpha_m = 5.3 \times 10^{-5}$ K^{-1}. The variation of material properties is caused by varying volume fraction. Variation of the fibre's volume fraction has been chosen as the polynomial function of x, y.

- Part 1

$$\begin{aligned} v_f(x,y) =& 1/10 + 220 \times 10^3 x^2 - 232 \times 10^6 x^3 + 73600 \times 10^6 x^4 - 6912 \times 10^9 x^5 \\ & - 112 \times 10^{12} x^2 y^2 + 108800 \times 10^{12} x^3 y^2 - 33280 \times 10^{15} x^4 y^2 \\ & + 3072 \times 10^{18} x^5 y^2 - 112 \times 10^{15} x^2 y^3 + 108800 \times 10^{15} x^3 y^3 \\ & - 33280 \times 10^{18} x^4 y^3 + 3072 \times 10^{21} x^5 y^3 + 22400 \times 10^{18} x^2 y^4 \\ & - 21760 \times 10^{21} x^3 y^4 + 6656000 \times 10^{21} x^4 y^4 - 614400 \times 10^{24} x^5 y^4 \\ & + 44800 \times 10^{21} x^2 y^5 - 43520 \times 10^{24} x^3 y^5 + 13312 \times 10^{27} x^4 y^5 \\ & - 1228800 \times 10^{27} x^5 y^5 \end{aligned}$$

- Part 2

$$v_f(x,y) = 0.766683$$

- Part 3

$$\begin{aligned} v_f(x,y) =& 0.766683 + 4.26633 \times 10^6 x^2 - 1.84858 \times 10^{10} x^3 + 3.89101 \times 10^{13} x^4 \\ & - 4.99269 \times 10^{16} x^5 + 4.25073 \times 10^{19} x^6 - 2.49749 \times 10^{22} x^7 \\ & + 1.0285 \times 10^{25} x^8 - 2.96182 \times 10^{27} x^9 + 5.83847 \times 10^{29} x^{10} \\ & - 7.49901 \times 10^{31} x^{11} + 5.64709 \times 10^{33} x^{12} - 1.88879 \times 10^{35} x^{13} \end{aligned}$$

Variation of the fibres volume fraction $v_f(x,y)$ for part 1 and 3 are shown in Figure 3. The same variation of the fibres volume fraction at the points B and C has been assumed.

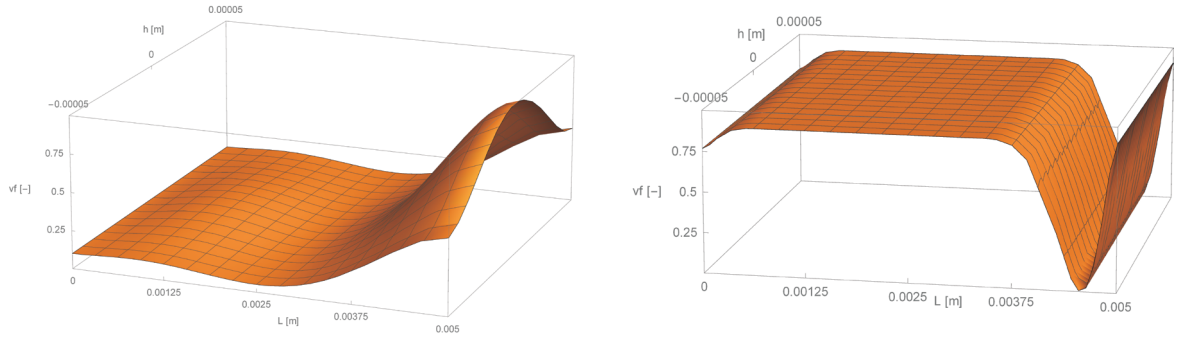

Figure 3: Variation of the fibres volume fraction, left - part 1, right - part 3

The effective material properties (Young modulus for tension/compression $E_L^{NH}(x)$ [Pa], Young modulus for bending $E_L^{MH}(x)$ [Pa], thermal conductivity $\lambda_L^H(x)$ [$\mathrm{Wm^{-1}K^{-1}}$], electric conductivity $\rho_L^H(x)$ [S/m], thermal expansion coefficient α_{TL}^H [$\mathrm{K^{-1}}$]) of the homogenized beam have been calculated by multilayered method [2], [3] and the results are:

- Beam 1 (the local axis x begins at node A and ends at point B - see Fig. 2):

$$\begin{aligned} E_L^{NH} =& 2.695 \times 10^{11} + 2.24267 \times 10^{16} x^2 - 2.44373 \times 10^{19} x^3 \\ & + 7.85707 \times 10^{21} x^4 - 7.424 \times 10^{23} x^5 \end{aligned}$$

$$\begin{aligned} E_L^{MH} =& 2.695 \times 10^{11} + 1.70473 \times 10^{8} x + 1.62396 \times 10^{16} x^2 \\ & - 1.84272 \times 10^{19} x^3 + 6.01868 \times 10^{21} x^4 - 5.72704 \times 10^{23} x^5 \end{aligned}$$

$$\begin{aligned} \lambda_L^H =& 106 + \frac{135868725000}{14641} x^2 - \frac{148050030000000}{14641} x^3 \\ & + \frac{47600892000000000}{14641} x^4 + \frac{4497721920000000000}{14641} x^5 \end{aligned}$$

$$\begin{aligned} \rho_L^H =& 1.463 \times 10^{7} + 2.3664 \times 10^{12} x^2 - 2.57856 \times 10^{15} x^3 \\ & + 8.29057 \times 10^{17} x^4 - 7.83361 \times 10^{19} x^5 \end{aligned}$$

$$\begin{aligned}\alpha_{TL}^{H} =& 0.00001356 - 0.000286032x - 1.52203x^2 + 1923.69x^3 \\ & - 649717x^4x^5 - 6.34908 \times 10^7 x^5\end{aligned}$$

- Beam 2 (the local axis x begins at node B and ends at point C - see Fig. 2):

$$E_L^{NH} = 3.66169 \times 10^7$$

$$E_L^{MH} = 3.66169 \times 10^7$$

$$\lambda_L^{H} = 146.001$$

$$\rho_L^{H} = 2.48302 \times 10^7$$

$$\alpha_{TL}^{H} = 0.0000118$$

- Beam 3 (the local axis x begins at node C and ends at point D - see Fig. 2):

$$\begin{aligned}E_L^{NH} =& 3.66169 \times 10^{11} + 6.18618 \times 10^{17}x^2 - 2.68044 \times 10^{21}x^3 \\ & + 5.64197 \times 10^{24}x^4 - 7.2394 \times 10^{27}x^5 + 6.16356 \times 10^{30}x^6 \\ & - 3.62135 \times 10^{33}x^7 + 1.49132 \times 10^{36}x^8 - 4.29464 \times 10^{38}x^9 \\ & + 8.46578 \times 10^{40}x^{10} - 1.08736 \times 10^{43}x^{11} + 8.18829 \times 10^{44}x^{12} \\ & - 2.73875 \times 10^{46}x^{13}\end{aligned}$$

$$\begin{aligned}E_L^{MH} =& 3.66169 \times 10^{11} + 6.18618 \times 10^{17}x^2 - 2.68044 \times 10^{21}x^3 \\ & + 5.64197 \times 10^{24}x^4 - 7.2394 \times 10^{27}x^5 + 6.16356 \times 10^{30}x^6 \\ & - 3.62135 \times 10^{33}x^7 + 1.49132 \times 10^{36}x^8 - 4.29464 \times 10^{38}x^9 \\ & + 8.46578 \times 10^{40}x^{10} - 1.08736 \times 10^{43}x^{11} + 8.18829 \times 10^{44}x^{12} \\ & - 2.73875 \times 10^{46}x^{13}\end{aligned}$$

$$\begin{aligned}\lambda_L^{H} =& 146.001 + 2.5598 \times 10^{8}x^2 - 1.10915 \times 10^{12}x^3 \\ & + 2.33461 \times 10^{15}x^4 - 2.99561 \times 10^{18}x^5 + 2.55044 \times 10^{21}x^6 \\ & - 1.49849 \times 10^{24}x^7 + 6.17099 \times 10^{26}x^8 - 1.77709 \times 10^{29}x^9 \\ & + 3.50308 \times 10^{31}x^{10} - 4.49941 \times 10^{33}x^{11} + 3.38826 \times 10^{35}x^{12} \\ & - 1.13328 \times 10^{37}x^{13}\end{aligned}$$

$$\begin{aligned}\rho_L^{H} =& 2.48302 \times 10^{7} + 6.52749 \times 10^{13}x^2 - 2.82832 \times 10^{17}x^3 \\ & + 5.95325 \times 10^{20}x^4 - 7.63882 \times 10^{23}x^5 + 6.50362 \times 10^{26}x^6 \\ & - 3.82115 \times 10^{29}x^7 + 1.5736 \times 10^{32}x^8 - 4.53158 \times 10^{34}x^9 \\ & + 8.93286 \times 10^{36}x^{10} - 1.14735 \times 10^{39}x^{11} + 8.64006 \times 10^{40}x^{12} \\ & - 2.88985 \times 10^{42}x^{13}\end{aligned}$$

$$\alpha_{TL}^{H} = 6.87608 \times 10^{-6} - 0.000186889x$$

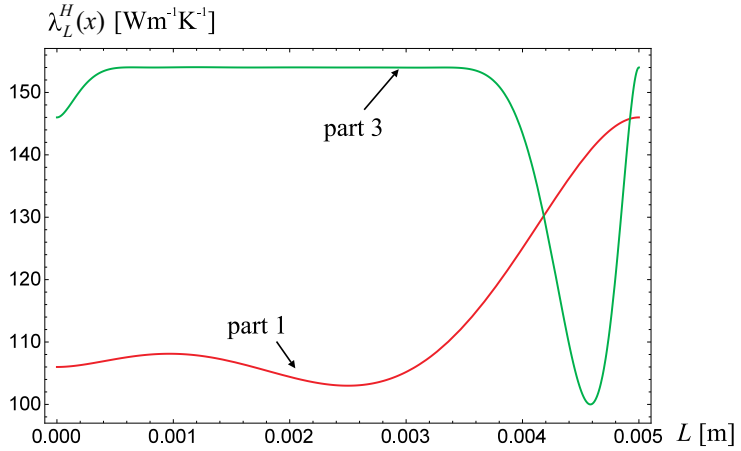

Figure 4: Homogenized thermal conductivity

The homogenized thermal conductivity $\lambda_L^H(x)$ at part 1 and 3 is shown in Fig. 4.

The applied constrains and loads:

- electric potential and current: $V_A = 0$ V, $I_D = 5$ A;
- temperatures: $T_A = 25$ °C, TD = 25 °C;
- fixed support: $u_A = 0$ m, $u_D = 0$ m,
  $w_A = 0$ m, $w_D = 0$ m,
  $\varphi_A = 0$ rad, $\varphi_D = 0$ rad;

The coupled electro-thermo-mechanical analysis of FGM actuator has been done using our new FGM beam/link finite elements. The calculation has been done using software MATHEMATICA [5]. Only three our new finite elements have been used (one for each part). The same problem has been solved using a fine mesh - 12998 of PLANE223 elements of the FEM program ANSYS [6]. The average relative difference Δ [%] between quantities calculated by our method and the ANSYS solution has been evaluated.
Electric analysis was performed as the first solution and the nodal electric variables φ have been obtained (see Table 1).

Table 1: The results of electric analysis

electric potential [V]	new element	ANSYS	Δ [%]
φ_B	0.077782	0.0775569	0.28
φ_C	0.080298	0.0796372	0.82
φ_D	0.131995	0.131098	0.67

Thermal analysis was performed as the second one. Distributed thermal load - Joule heat caused by electric current, was included into the analysis. The results of thermal alalysis are presented in Table 2.

Table 2: The results of thermal analysis

temperature [°C]	new element	ANSYS	Δ [%]
T_B	346.33	340.42	1.71
T_C	342.08	336.77	1.55

Structural analysis is performed as the last analysis, where thermal forces caused by thermal expansion were included into the model. The solution of structural analysis are the displacements u for longitudinal direction and w for transversal direction (see Table 3).

Table 3: The results of structural analysis

displacement [m]	new element	ANSYS	Δ [%]
u_B	0.13713 $\times 10^{-4}$	0.13588 $\times 10^{-4}$	0.91
w_B	-0.70975 $\times 10^{-4}$	-0.72665 $\times 10^{-4}$	2.38
u_C	0.67744 $\times 10^{-5}$	0.65903 $\times 10^{-5}$	2.71
w_C	-0.71917 $\times 10^{-4}$	-0.73204 $\times 10^{-4}$	1.78

As it can be seen in Tables 1 - 3, a very good agreement of both solution results has been obtained. The comparison of total deformation of the FGM actuator calculated by our new approach and comercial FEM program ANSYS is shown in Fig. 5.

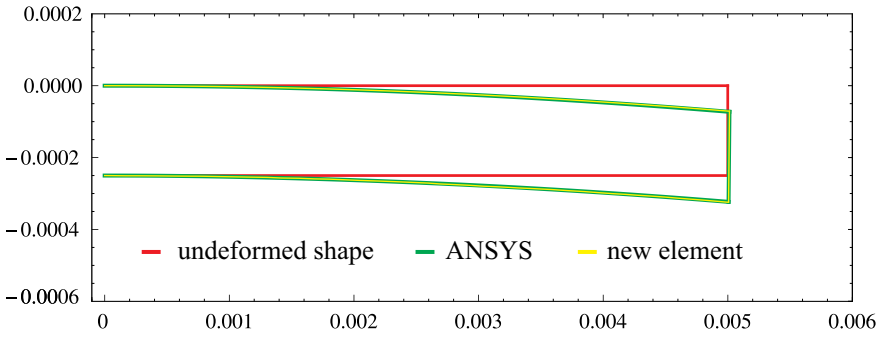

Figure 5: Total deformation of the FGM actuator

4 CONCLUSIONS

New FEM equations for weak coupled static electro-thermo-mechanical analysis of the FGM beam structures have been presented in this contribution. The numerical experiment – multiphysical analysis of micro actuator made of FGM has been done using our new approach and obtained results have been compared with ones obtained by solution with software ANSYS. The effectiveness and accuracy of the new finite elements have been shown.

Acknowledgement: This paper has been supported by Grant Agency APVV-0246-12, Grant Agency VEGA No. 1/0228/14, Grant Agency VEGA No. 1/0453/15 and Agency KEGA No. 007STU-4/2015.

REFERENCES

[1] Murín, J., Kutiš, V. *Improved mixture rules for composite (FGMs) sandwich beam finite element.* In Computational Plasticity IX. Fundamentals and Applications. Barcelona, Spain, (2007): 647-650.

[2] Kutiš, V., J. Murín, J., Belák, R. and Paulech, J. *Beam element with spatial variation of material properties for multiphysics analysis of functionally graded materials.* Computers and Structures, 89:11921205, 2011.

[3] Murín, J., Kutiš, V., Paulech, J. and Hrabovský, J. *Electric-Thermal Link Finite Element Made of a FGM with Spatial Variation of Material Properties.* Composites Part B: Engineering, 42:19661979, 2011.

[4] Rubin, H. *Solution of differential equations of arbitrary order with polynomial coefficients and application to a statics problem.* ZAMM 76 (1996), 105-117.

[5] S. Wolfram MATHEMATICA 5, Wolfram research, Inc., 2003.

[6] ANSYS Swanson Analysis System, Inc., 201 Johnson Road, Houston, PA 15342/1300, USA.